

Ferroelectric phase transition in deuterated glycinium phosphite crystals

J. Baran and M. Śledź

Institute of Low Temperature and Structure Research, Polish Academy of Sciences, Okólna 2, 50-950 Wrocław 2, P.O. Box 937, Poland

R. Jakubas and G. Bator

Faculty of Chemistry, University of Wrocław, 50-383 Wrocław, Joliot Curie 14, Poland

(Received 22 July 1996)

The dielectric permittivity between 500 Hz and 1 GHz and pyroelectric properties of $(\text{ND}_3\text{CH}_2\text{COOD})\text{D}_2\text{PO}_3$ (DGPI) single crystals in the vicinity of ferroelectric phase transition (322 K) are measured. The spontaneous polarization along the b axis is found to be $5 \times 10^{-3} \text{ C/m}^2$ at 290 K. DGPI shows the critical slowing down near 322 K. The results confirm the order-disorder nature of the ferroelectric phase transition of the second order type. [S0163-1829(97)04901-1]

Glycinium phosphite crystals $[(\text{NH}_3\text{CH}_2\text{COOH})\text{H}_2\text{PO}_3]$, abbreviated as GPI] undergo continuous ferroelectric phase transition at 224 K.¹ It is the second ferroelectric crystal of the phosphorous acid with amino acids beside the betainium phosphite crystal $[(\text{CH}_3)_3\text{NCH}_2\text{COOHH}_2\text{PO}_3]$, abbreviated as BPI.² Both these crystals belong to the monoclinic system and similar space group ($P2_1/a$ and $P2_1/c$ for GPI and BPI, respectively). Their structures contain the infinite chains of hydrogen bonded phosphite anions to which the amino acid cations are attached by strong hydrogen bonds.^{3,4} These chains are oriented parallel and perpendicularly to the ferroelectric b axis in BPI and GPI, respectively.

Very large isotopic effect (ca. 100 K) on the T_c indicates the essential role of the strong interphosphite hydrogen bonds in the paraelectric-ferroelectric phase transition mechanism of both the BPI (Ref. 5) and GPI (Ref. 6) crystals. According to the x-ray data these hydrogen bonds are centrosymmetric with disordered protons^{3,4} in the paraelectric phase. That seems to be in accordance with the dielectric measurement. The investigation of the dielectric relaxation indicates that the ferroelectric dynamics of the BPI crystal⁷ is described in terms of the soft relaxational mode associated with the proton flipping motion in the double potential well. The activation energy ($\Delta E = 17 \text{ kJ/mol}$) estimated for the GPI crystal is, however, more than three times higher than that obtained for BPI ($\Delta E = 5 \text{ kJ/mol}$). Simultaneously, the macroscopic relaxation time in the GPI crystal ($\tau = 4 \times 10^{-10} \text{ s}$ at temperature close to the T_c) is nearly one order in magnitude longer than that ($\tau = 6.6 \times 10^{-11} \text{ s}$) found in BPI.⁸ This implies that the mechanism of the paraferroelectric phase transition in the GPI crystals is not only strictly connected with the movements of the protons in the strong interphosphite hydrogen bonds. Thus it might be suggested that the dynamics of the organic sublattice (glycinium cations) of GPI could play a key role in the long-range order. Most likely, the dynamical disorder of the protons is coupled to the motions of the glycinium cations. Accordingly, only one type of the glycinium cations is observed by the vibrational methods in the paraelectric phase. In the ferroelectric phase a splitting of some glycinium bands is observed.⁶ It may indicate that two different glycinium cations appear in the ferroelectric phase. Thus it seems that the spontaneous

polarization is due to the ordering of the glycinium cations which force the protons into order in the interphosphite hydrogen bonds. The knowledge of the dielectric properties of the deuterated crystal, $(\text{ND}_3\text{CH}_2\text{COOD})\text{D}_2\text{PO}_3$, will allow one to determine more precisely the nature of the paraelectric-ferroelectric phase transition in the GPI crystal. This is the subject of this paper.

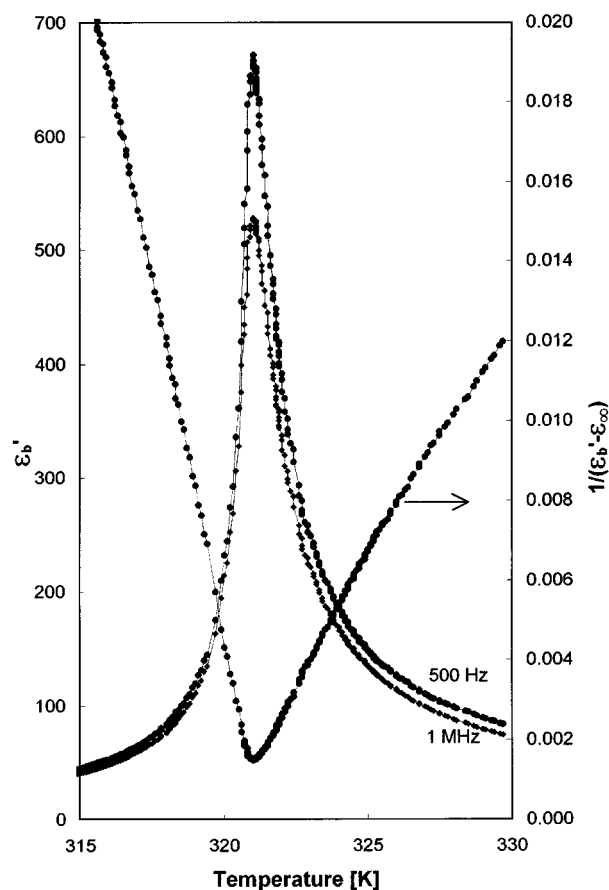


FIG. 1. Temperature dependence of the real part of complex electric permittivity, ϵ' , in the vicinity of $T_c = 322 \text{ K}$ at 500 Hz and 1 MHz and illustration of the Curie-Weiss law along the b axis for the DGPI crystal at 500 Hz.

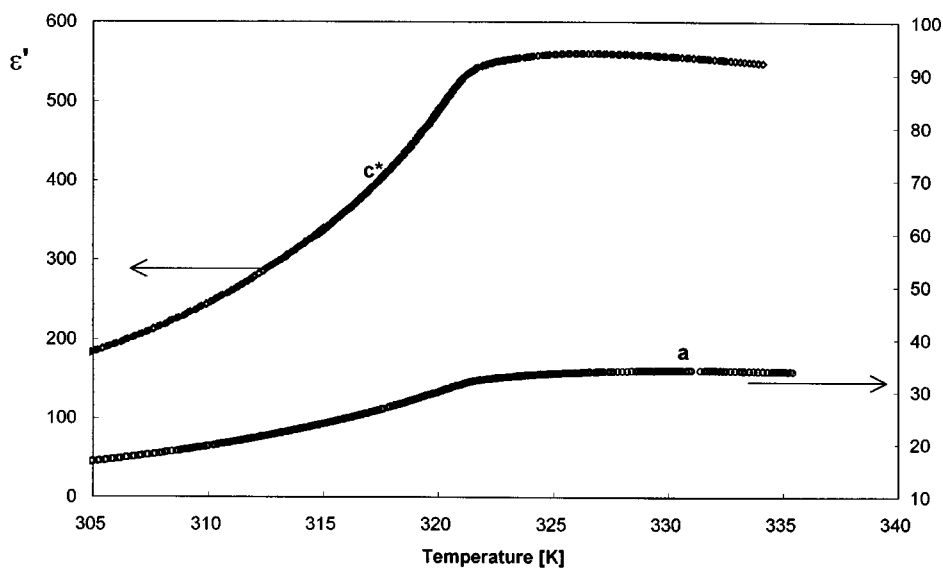


FIG. 2. Electric permittivity vs temperature measured along the c^* and a axes for the DGPI crystal.

The GPI crystals were grown from the aqueous solutions containing the glycine and phosphorous acid in the ratio 1:1. The deuterated crystals were obtained by threefold recrystallization from a solution in the D_2O (99.8%). In each step of crystallization 48 g of GPI were dissolved in 50 ml of hot D_2O . The estimated value (from the IR and Raman powder spectra in Ref. 6) of a deuterium concentration is more than 95% for the protons attached to nitrogen (NH_3) and oxygen (OH) atoms and ca. 65% for the P-H bonds.

For the dielectric measurements, the samples of dimensions $5 \times 5 \times 1$ mm³ were cut perpendicularly to the a , b , and c^* direction. The plates were silver painted. Complex electric permittivity was measured by a HP 4284A Precision LCR Meter in the frequency range 500 Hz–1 MHz and by a HP 4191A Impedance Analyzer in the frequency range 30 MHz–1 GHz. The measurements were performed in the temperature range 290–350 K on heating. The temperature of the specimen was varied continuously with the rate of 0.1 K/min in the vicinity of T_c and 0.5 K/min elsewhere. In the high frequency region the temperature was stabilized and

controlled by a UNIPAN Temperature Controller type 650 with fluctuation less than ± 0.1 K. The overall error for complex electric permittivity was less than 5% and 10% in the low and high frequency region, respectively.

The measurements of the pyroelectric current and charge were performed under short-circuit conditions during linear heating of the sample (with a rate of 1 K/min) on a Keithley 617 type electrometer. For the pyroelectric studies, the silver painted area (about 9.5 mm²) of the samples was perpendicular to the b axis. The reproducibility of the pyroelectric current was better than 20% for all samples and the experimental error of ΔP_s was smaller than $1 \mu C/m^2$.

The temperature dependence of the real part of the complex electric permittivity (ϵ') for DGPI taken at 500 Hz and 1 MHz is shown in Fig. 1. A pronounced λ -type peak of ϵ' is found along the b direction at $T_c = 322$ K ($\epsilon'_{max} = 680$ at 500 Hz and 530 at 1 MHz). Except for the close vicinity of T_c , the dielectric dispersion is not observed up to 1 MHz both for the paraelectric and ferroelectric phase, whereas, in the case of the GPI crystals, a distinct low-frequency disper-

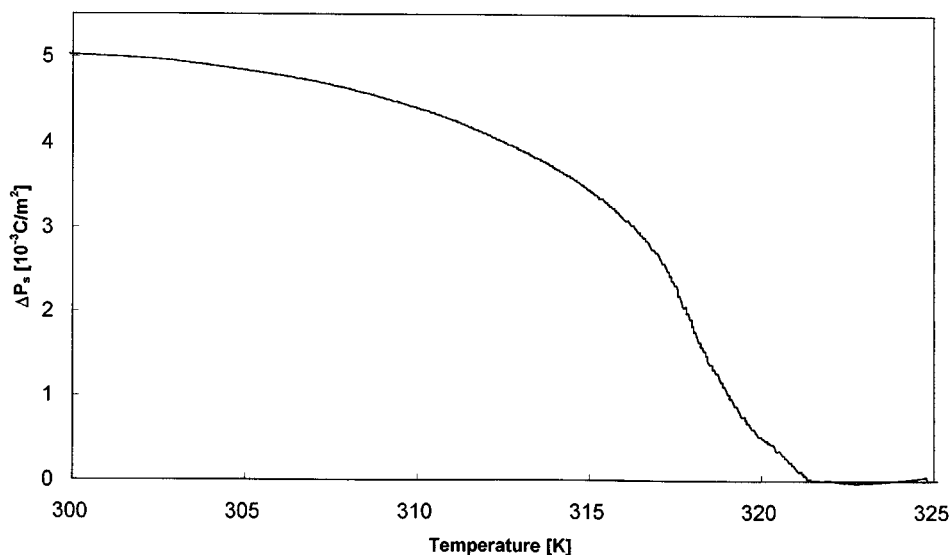


FIG. 3. Change of the spontaneous polarization, ΔP_s , as a function of temperature for the DGPI crystal.

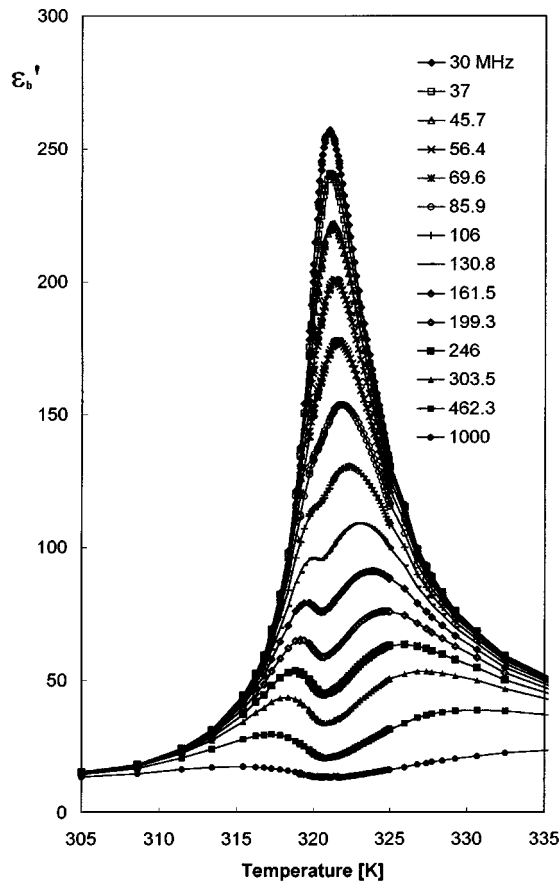


FIG. 4. Temperature dependence of the real part of complex electric permittivity, ϵ'_b , in the vicinity of $T_c=322$ K for several frequencies along the b axis for the DGPI crystal.

sion appears in the ferroelectric phase due to the domain-walls motion.¹ In a temperature range of about 10 K above T_c , the temperature dependence of ϵ'_b measured at 500 Hz is well represented by the Curie-Weiss relation $\epsilon' = \epsilon_\infty + C_+ / (T - T_0)$ (see Fig. 1). The parameters of this

relation determined by the least-squares fitting are the following: $\epsilon_\infty = 10$, $T_0 = 320$ K, and $C_+ = 705$ K (whereas below T_c , $C_- = 265$ K). The ratio of Curie-Weiss constants above and below T_c , $C_+ / C_- = 2.66$, is typical for ferroelectric crystals with continuous phase transition. The value of C_+ is also characteristic of the ferroelectrics with the order-disorder type of phase transition. We should also notice that deuteration strongly influences the Curie-Weiss value (C_+) which in the case of GPI was found to be 260 K.⁶

Electric permittivity vs temperature measured along the c^* and a axis is shown in Fig. 2 (the c^* direction is perpendicular to the a axis). In general, the electric anisotropy both in the GPI and DGPI crystals reveals large similarity. However, the deuteration causes a distinct increase in the ϵ_{c^*} value, which is nearly twice as large as that observed in GPI. It is interesting that the ϵ_{c^*} value in the vicinity of T_c is comparable with those found for the polar b axis of the title crystal. We should notice, however, that the shape of the $\epsilon_{c^*}(T)$ curve is rather unusual. The value of ϵ_{c^*} is quite large even for the temperature far from T_c ($\epsilon_{c^*} = 180$ at 305 K) and increases substantially to 550 units at T_c . This high value of ϵ_{c^*} is preserved more or less constant in the measured temperature range of the paraelectric phase.

The temperature dependence of the pyroelectric charge was measured along the b axis in order to check the ferroelectric activity. As shown in Fig. 3, the pyroelectric signal appears below 322 K. These measurements were performed after the sample had been cooled to room temperature under an applied dc electric field of about 2.5 kV/cm. The spontaneous polarization P_s at room temperature was about 5×10^{-3} C/m². The observation of the 50 Hz $D-E$ loop at room temperature additionally confirmed the ferroelectric nature of the low temperature (below 322 K) phase. The value of the P_s found in DGPI is nearly the same as that in the case of GPI.

Figure 4 shows the temperature dependence of the real part of complex electric permittivity, ϵ'_b , in the vicinity of $T_c = 322$ K for several frequencies between 30 and 1000 MHz measured along the b axis. ϵ'_b shows a peak at 322 K

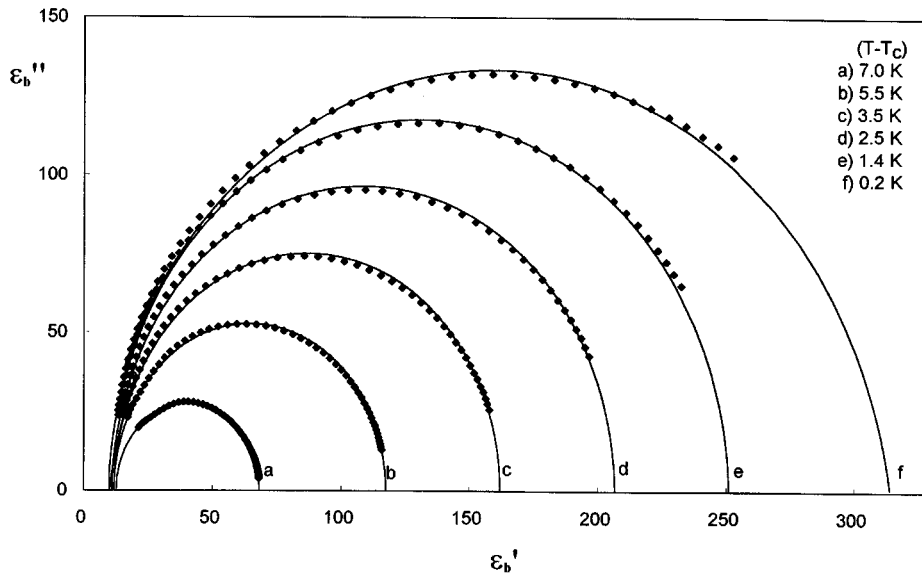


FIG. 5. The Cole-Cole diagram in the paraelectric phase for the DGPI crystal.

up to 100 MHz and above this frequency it splits into two peaks, the width of which broadens with increasing frequency.

The Cole-Cole plots of the observed relaxation are presented in Fig. 5. The dielectric relaxation in DGPI crystals is well described by the following Cole-Cole relation:

$$\varepsilon^* = \varepsilon_\infty + (\varepsilon_0 - \varepsilon_\infty) / [1 + (i\omega\tau)^{1-\alpha}], \quad (1)$$

where ε_0 and ε_∞ are low and high frequency limits of the electric permittivity, respectively, ω is angular frequency, τ is relaxation time, and α is distribution of relaxation times parameter. ε_0 , ε_∞ , τ , and α are the fit parameters for each temperature independently. The small values of α ($\alpha < 0.02$) indicate the almost monodispersive nature of dielectric relaxation in DGPI.

The results presented in Figs. 4 and 5 indicate that the fundamental ferroelectric dispersion appears in the microwave frequency region. On approaching the Curie temperature, the macroscopic relaxation time reaches the value of

2.2×10^{-9} s. This value is comparable with that obtained for other hydrogen bonded ferroelectrics like TGS—family crystals,⁹ CDP,¹⁰ and RbD₂PO₄.¹¹

The results of dielectric dispersion presented above are characteristic of the para-ferroelectric phase transition of the second order type, where a critical slowing down of the macroscopic relaxation time (τ) is observed. The relaxational mode softens to the frequency of 75 MHz at T_c , which is more than three times lower than that (250 MHz) in the normal GPI crystal.

Now it may be concluded that deuteration of the GPI crystal influences its dynamical properties in the vicinity of the para-ferroelectric phase transition temperature. This manifests itself by the elongation of the macroscopic relaxation time on deuteration even when taking into account that the temperature of the phase transition (T_c) is higher for DGPI (322 K) than for GPI (225 K).

This work was supported by KBN project register No. 2P 303 110 06.

¹S. Dacko, Z. Czapla, J. Baran, and M. Drozd, Phys. Lett. (to be published).

²J. Albers, A. Klöpperpierper, H. J. Rother, and S. Haussühl, Ferroelectrics **81**, 27 (1988).

³I. Fehst, M. Paasch, S. L. Hutton, M. Braune, R. Brohmer, A. Loidl, R. Dorffer, T. T. Narz, S. Haussühl, and G. J. McIntyre, Ferroelectrics **138**, 1 (1993).

⁴M. T. Averbuch-Pouchot, Acta Crystallogr. C **49**, 815 (1993).

⁵S. Launer, M. Le Maire, G. Schaack, and S. Haussühl, Ferroelectrics **132**, 257 (1992).

⁶J. Baran, G. Bator, R. Jakubas, and M. Śledź, J. Phys. Condens. Matter (to be published).

⁷R. Sobiestianskas, J. Grigas, Z. Czapla, and S. Dacko, Phys. Status Solidi A **136**, 223 (1993).

⁸G. Koch and H. Happ, Ann. Phys. (Leipzig) **2**, 522 (1993).

⁹K. Takayama, K. Deguchi, and E. Nakamura, J. Phys. Soc. Jpn. **53**, 4121 (1984).

¹⁰E. Kanda, A. Tamaki, and T. Fujimura, J. Phys. C **15**, 3401 (1982).

¹¹M. Komukae and Y. Makita, J. Phys. Soc. Jpn. **54**, 4359 (1985).